Development of Surge Simulation Code Based on Finite-Difference Time-Domain (FDTD) Approximation of Maxwell's Equations

Taku Noda and Shigeru Yokoyama
CRIEPI - Central Research Institute of Electric Power Industry
2-11-1 Iwado-kita, Komae-shi, Tokyo, 201-8511, Japan
takunoda@criepi.denken.or.jp, yokoyama@criepi.denken.or.jp

Abstract – **This paper presents the development of a surge analysis program named VSTL (Virtual Surge Test Lab.) based on the Maxwell Equations formulated by the FDTD (finite-difference time-domain) method. By use of the Maxwell Equations, VSTL is inherently able to take into account the three-dimensional geometrical features of a simulated structure unlike EMTP-type circuit-based transient programs. In terms of the handling of imperfectly-conducting medium such as earth soil, VSTL is more advantageous than MoM (method of moments) based programs such as NEC-2. This paper also presents comparisons between calculated and measured results to validate the accuracy of VSTL.**

Keywords : Maxwell's Equations, FDTD method, surge analysis, three-dimensional circuit, imperfectly conducting medium, thin wire.

I. INTRODUCTION

The processing speed and the memory capacity of computers have rapidly been progressing, and the FDTD (finite-difference time-domain) method that solves the Maxwell Equations by the method of difference becomes a practical choice in the field of antenna analysis [1, 2]. In the field of surge analysis, the FDTD method was applied to the analysis of transient grounding resistance [3]. At present, even a personal computer can be used for the FDTD analysis, and this circumstance occurs to the authors to develop a surge analysis program based on the FDTD method.

This paper describes the development of a surge analysis program named VSTL (Virtual Surge Test Lab.) based on the FDTD method. VSTL has been developed by the authors from scratch at CRIEPI since late 1999, and continuous development is being carried out. VSTL is one of the registered programs of CRIEPI which are available to Japanese electric power utilities and to non-profitable research groups in the world. The FDTD method divides the space of interest into cubic cells and directly calculates the electric and magnetic fields of the cells by discretizing the Maxwell Equations, where the derivatives with respect to time and space are replaced by a numerical difference. Updating the procedure at each timestep gives the transient solution of electric and magnetic fields. By use of the FDTD method, the developed program is inherently able to take into account the geometrical features of a simulated structure, unlike EMTP-type circuit-based transient programs. Thus, the program is advantageous to solve both the following problem types:

(i) surge propagation on a three-dimensional circuit (three-dimensional skeleton structure)
(ii) surge propagation inside a three-dimensional imperfectly conducting medium such as earth soil.

The method of moments (MoM) also numerically solves the Maxwell Equations [4], and NEC-2 is a well-known program based on MoM [5]. Although MoM efficiently solves the type (i) problems, it cannot solve the type (ii) ones except very simple cases, because the handling of three-dimensional current distribution in the imperfectly conducting medium is complicated [6]. On the other hand, FDTD is inherently able to solve both the problem types efficiently. One weak point of FDTD is the treatment of a thin wire. Thus, a field correction method to accurately treat the radius of the thin wire is proposed in a companion paper [7] and implemented in VSTL. In this paper, the solution method of VSTL is first described, and benchmark simulation results compared with experimental ones are presented.

II. ALGORITHM

In the analysis of VSTL, the analysis space is defined as a rectangular-parallelepiped space. Arbitrary number of thin-wire conductors, rectangular-parallelepiped conductors, and localized voltage and current sources are arbitrarily placed in the analysis space, and transient electric and magnetic fields are calculated. The bottom of the analysis space can be defined as an imperfectly-conducting medium such as earth, and each boundary of the analysis space can independently be defined as a perfectly-conducting plane or an absorbing plane. The waveform of a localized voltage or current at an arbitrary position is outputted as specified. Animation of electric or magnetic field distribution in an arbitrary section is generated by transferring data to MATLAB.

A. FDTD Formulation [1, 2]

The Maxwell Equations in the Cartesian coordinates are as follows assuming no anisotropic and/or dispersive medium in the space of interest.

$$\nabla \times \boldsymbol{E} = -\mu \frac{\partial \boldsymbol{H}}{\partial t}, \quad \nabla \times \boldsymbol{H} = \varepsilon \frac{\partial \boldsymbol{E}}{\partial t} + \sigma \boldsymbol{E} \tag{1}$$

$$\nabla \cdot \boldsymbol{E} = \rho / \varepsilon, \quad \nabla \cdot \boldsymbol{H} = 0 \tag{2}$$

where $\boldsymbol{E}$: electric field, $\boldsymbol{H}$: magnetic field, ρ : charge density, ε : permittivity, μ : permeability, σ : conductivity, and all the quantities are in MKSA units. Discretizing the analysis space by a small length Δs in all the directions, the space is filled with cubes of which the sides are Δs, and the cube is called "cell". Assume that the number of divisions of the analysis space along the x coordinate is N_x, along the y coordinate N_y, and along the z coordinate N_z. The analysis space is given by the following range.

$$x = i\Delta s, (0 \le i \le N_x), \quad y = j\Delta s, (0 \le j \le N_y), \\ z = k\Delta s, (0 \le k \le N_z) \tag{3}$$

Equation (1) includes derivatives with respect to position x, y, z, and time t. In the FDTD formulation, representing values of electric and magnetic fields in a cell is configured by turns as shown in Fig. 1, and this yields the replacement of the derivatives with respect to x, y, and z in (1) with the following central difference.

$$\frac{\partial f(x)}{\partial x} \cong \frac{f(x+\Delta s/2) - f(x-\Delta s/2)}{\Delta s} \tag{4}$$

In the above equation, f is a component of $\boldsymbol{E}$ or $\boldsymbol{H}$, and the same equation is valid also to y and z. The same central difference shown in the following equation replaces the derivatives with respect to time in (1), assuming that electric fields are calculated at time steps $t = n\Delta t$ (n = 0, 1, ⋯) and magnetic fields at $t = (n + 1/2)\Delta t$ (n = 0, 1, ⋯) by turns.

$$\frac{\partial f(t)}{\partial t} \cong \frac{f(t+\Delta t/2) - f(t-\Delta t/2)}{\Delta t} \tag{5}$$

Applying (4) and (5) to (1) yields the following difference equations (e.g. $E^n{}_x(i + 1/2, j, k)$ represents x component electric field at position $x = (i + 1/2)\Delta s$, $y = j\Delta s$, $z = k\Delta s$, and at time $t = n\Delta t$, and the other components are expressed in the same manner).

$$E_x^n(i+\tfrac{1}{2},j,k) = K_1 E_x^{n-1}(i+\tfrac{1}{2},j,k) \\ + K_2\{H_z^{n-1/2}(i+\tfrac{1}{2},j+\tfrac{1}{2},k) - H_z^{n-1/2}(i+\tfrac{1}{2},j-\tfrac{1}{2},k) \\ - H_y^{n-1/2}(i+\tfrac{1}{2},j,k+\tfrac{1}{2}) + H_y^{n-1/2}(i+\tfrac{1}{2},j,k-\tfrac{1}{2})\} \tag{6}$$

$$E_y^n(i,j+\tfrac{1}{2},k) = K_1 E_y^{n-1}(i,j+\tfrac{1}{2},k) \\ + K_2\{H_x^{n-1/2}(i,j+\tfrac{1}{2},k+\tfrac{1}{2}) - H_x^{n-1/2}(i,j+\tfrac{1}{2},k-\tfrac{1}{2}) \\ - H_z^{n-1/2}(i+\tfrac{1}{2},j+\tfrac{1}{2},k) + H_z^{n-1/2}(i-\tfrac{1}{2},j+\tfrac{1}{2},k)\} \tag{7}$$

$$E_z^n(i,j,k+\tfrac{1}{2}) = K_1 E_z^{n-1}(i,j,k+\tfrac{1}{2}) \\ + K_2\{H_y^{n-1/2}(i+\tfrac{1}{2},j,k+\tfrac{1}{2}) - H_y^{n-1/2}(i-\tfrac{1}{2},j,k+\tfrac{1}{2}) \\ - H_x^{n-1/2}(i,j+\tfrac{1}{2},k+\tfrac{1}{2}) + H_x^{n-1/2}(i,j-\tfrac{1}{2},k+\tfrac{1}{2})\} \tag{8}$$

$$H_x^{n+1/2}(i,j+\tfrac{1}{2},k+\tfrac{1}{2}) = H_x^{n-1/2}(i,j+\tfrac{1}{2},k+\tfrac{1}{2}) \\ + K_3\{-E_z^n(i,j+1,k+\tfrac{1}{2}) + E_z^n(i,j,k+\tfrac{1}{2}) \\ + E_y^n(i,j+\tfrac{1}{2},k+1) - E_y^n(i,j+\tfrac{1}{2},k)\} \tag{9}$$

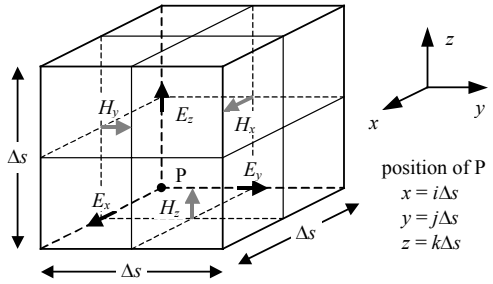

Fig. 1 Configuration of electric and magnetic fields in cell

$$H_y^{n+1/2}(i+\tfrac{1}{2},j,k+\tfrac{1}{2}) = H_y^{n-1/2}(i+\tfrac{1}{2},j,k+\tfrac{1}{2}) \\ + K_3\{-E_x^n(i+\tfrac{1}{2},j,k+1) + E_x^n(i+\tfrac{1}{2},j,k) \\ + E_z^n(i+1,j,k+\tfrac{1}{2}) - E_z^n(i,j,k+\tfrac{1}{2})\} \tag{10}$$

$$H_z^{n+1/2}(i+\tfrac{1}{2},j+\tfrac{1}{2},k) = H_z^{n-1/2}(i+\tfrac{1}{2},j+\tfrac{1}{2},k) \\ + K_3\{-E_y^n(i+1,j+\tfrac{1}{2},k) + E_y^n(i,j+\tfrac{1}{2},k) \\ + E_x^n(i+\tfrac{1}{2},j+1,k) - E_x^n(i+\tfrac{1}{2},j,k)\} \tag{11}$$

In the derivation of the above equations, an approximation $\sigma \boldsymbol{E}^{n-1/2} \cong \sigma\{\boldsymbol{E}^{n-1} + \boldsymbol{E}^n\}/2$ is used, and coefficients K_1, K_2, and K_3 are given by the following equations.

$$K_1 = \frac{1-\frac{\sigma\Delta t}{2\varepsilon}}{1+\frac{\sigma\Delta t}{2\varepsilon}}, \quad K_2 = \frac{\Delta t}{\varepsilon\Delta s}\frac{1}{1+\frac{\sigma\Delta t}{2\varepsilon}}, \quad K_3 = \frac{\Delta t}{\mu\Delta s} \tag{12}$$

Equations (6) – (11) are the FDTD formulas of the Maxwell Equations, and transient fields are obtained by calculating electric and magnetic fields by turns at time intervals $\Delta t/2$. Although (2) is not explicitly formulated, it is proofed that (6) – (11) automatically satisfies (2) [2]. The developed program VSTL uses this FDTD formulation.

B. Time Step Interval

Equations (6) – (11) are considered as numerical integration, and stable integration is performed if the following condition is satisfied (Courant's condition) [2].

$$\Delta t / \sqrt{\mu\varepsilon} \le \Delta s / \sqrt{3} \tag{13}$$

On the other hand, the grid dispersion error is minimized when the above relation is equated. Thus, the following formula is used in VSTL to determine time step interval Δt from user defined space step Δs.

$$\Delta t = \Delta s \sqrt{\mu\varepsilon/3}(1-\alpha) \tag{14}$$

α is a small positive value specified by a user in order to prevent instability of the numerical integration due to round-off error in (6) – (11).

C. Treatment of Boundaries

Each boundary of the analysis space can independently be defined as a perfectly-conducting plane or an absorbing plane

in VSTL. The perfectly-conducting plane can easily be represented by forcing the tangential components of electric fields at the boundary to be zero. VSTL uses second-order Liao's method to represent the absorbing plane, because it is more accurate and requires less memory compared with other methods [8]. An open space can be assumed by applying the absorbing plane to all the boundaries of the analysis space.

D. Imperfectly-Conducting Earth

The object of surge analysis is usually a three-dimensional skeleton structure above an imperfectly-conducting earth. In the analysis of VSTL, an imperfectly-conducting earth with arbitrary resistivity ρ_e can be defined at the bottom of the analysis space. The representation of the earth is simply accomplished by setting the value of σ in (12) to $1/\rho_e$ in the region defined as the earth soil. It is also possible, of course, to assume no earth in the analysis space.

E. Thin-Wire Conductors

Thin-wire conductors are one of the most fundamental components in surge analysis to represent power lines, steel frames, and so on. In order to represent the radius of such wires in a straightforward manner, the space step Δs has to be set to an extremely small value. But, in practice, the present computer resources do not allow such a small Δs (term "thin-wire conductor" or simply "thin wire" is used to indicate a conductive wire with a smaller radius than Δs in this paper as used in other papers).

Umashankar et al proposed a method to represent the radius of a thin wire with a reasonably large Δs, by correcting adjacent magnetic fields around the wire [9]. It is reported in [10] that this method is valid for antenna analysis. But, as described in section III-A in this paper, Umashankar's method does not give accurate surge impedance of a conductor which is a severe problem for surge analysis. Therefore, the authors proposed a new method correcting both the adjacent electric and magnetic fields around the wire. Because this new method is described in detail in a companion paper [7], only a brief description is given here.

In the FDTD analysis, the basic concept of thin wire representation is forcing the electric field along the center line of the wire to be zero as shown in Fig. 2 (a). Fig. 2 (b) is the cross section of the wire with the adjacent four electric fields, and Fig 2 (c) with the adjacent four magnetic fields. In order to take into account the effect of the thin-wire radius r, the new method uses the following corrected permittivity to calculate the adjacent four electric fields in (6) – (8).

$$\varepsilon' = m\varepsilon \text{ , (}\varepsilon\text{: permittivity of medium)} \tag{15}$$

And the following corrected permeability to calculate the adjacent four magnetic fields in (9) – (11).

$$\mu' = \mu / m \text{ , (}\mu\text{: permeability of medium)} \tag{16}$$

where m is given by

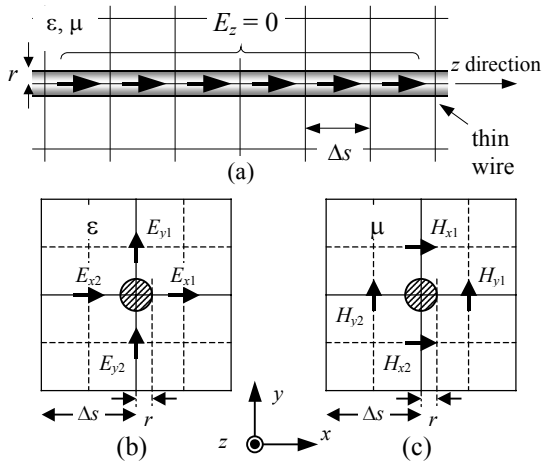

Fig. 2 Thin wire and configuration of adjacent electric and magnetic fields

$$m = \frac{1.471}{\ln(\Delta s / r)} . \tag{17}$$

Fig. 2 is an example thin wire along the z axis.

F. Rectangular-Parallelepiped Conductors

The geometrical shape of most power equipments can be represented by a combination of several rectangular-parallelepiped objects, and thus, a rectangular-parallelepiped conductor model is available in VSTL. The rectangular-parallelepiped conductor is simply modeled by forcing the tangential electric fields on its surface to be zero.

G. Localized Voltage and Current Sources

Unlike the static electric fields, the transient electric fields do not satisfy $\nabla \times \boldsymbol{E} = 0$. Thus, in the analysis of transient fields, the voltage or the voltage difference do not make sense in general. But, if we take notice of an electric field component of a cell, the voltage difference across a side of the cell can reasonably be defined as $V = E\Delta s$, because waves of which the wave length is shorter than $\lambda = 2\Delta s$ do not present in the FDTD calculation due to the bandwidth limitation of Δs. Therefore, we can model a localized voltage source by forcing an electric field component at a specified position in a specified direction to be a specified waveform. For example, in order to place a voltage source of which the waveform is given by $V^n = V(n\Delta t)$ at $x = i\Delta s$, $y = j\Delta s$, $z = (k + 1/2)\Delta s$ in the z direction, the following equation is used to force the electric field value.

$$E_z^n(i, j, k + \tfrac{1}{2}) = -\{V^n - RI^{n-1/2}\} / \Delta s \tag{18}$$

where R is the internal resistance of the voltage source specified by a user (it can be set to zero), and current I is given by the following equation as shown in Fig. 3.

$$\begin{aligned} I^{n-1/2} = \{&H_x^{n-1/2}(i, j - \tfrac{1}{2}, k + \tfrac{1}{2}) - H_x^{n-1/2}(i, j + \tfrac{1}{2}, k + \tfrac{1}{2}) \\ &+ H_y^{n-1/2}(i + \tfrac{1}{2}, j, k + \tfrac{1}{2}) - H_y^{n-1/2}(i - \tfrac{1}{2}, j, k + \tfrac{1}{2})\}\Delta s \end{aligned} \tag{19}$$

In the case of a current source, because current itself is a general quantity even in the transient fields, it can be modeled by modifying an electric field component at a specified position in a specified direction as in the following example. In order to place a current source of which the waveform is given by $I^n = I(n\Delta t)$ at $x = i\Delta s$, $y = j\Delta s$, $z = (k + 1/2)\Delta s$ in the z direction, the following term is added to (8).

$$-\frac{\Delta t/\varepsilon}{1+\frac{\sigma\Delta t}{2\varepsilon}}\frac{I^{n-1/2}}{\Delta s^2}, \text{ where } \sigma = 1/(R\Delta s), \tag{20}$$

and R is the internal resistance of the current source specified by a user (also, it can be set to zero).

H. Calculation Procedure and Output

The flow chart of the calculation procedure of VSTL is shown in Fig. 4. Localized voltage differences and current intensities at a specified position in a specified direction are included in the output of VSTL. The waveform of the localized voltage difference is calculated by $V = E\Delta s$, and that of the current intensity by (19). Animation of electric or magnetic field distribution in an arbitrary section is also included in the output. Electric field strength is calculated as the root-mean-square value of the two tangential components in the section, and magnetic field strength as the absolute value of the normal component in the section. The visualization is carried out by transferring data to MATLAB.

III. SIMULATION RESULTS

A. Horizontal Conductor System

A horizontal thin-wire conductor is one of the most fundamental elements of surge analysis. Fig. 5 shows a horizontal conductor system above a copper plate with radius r, height h, and length l = 4 m. The horizontal conductor is excited by a pulse generator (PG) of which the internal resistance is 50 Ω, and connected via a vertical wire. In this configuration, voltage and current waveforms at PG were measured, and simulations using VSTL were also carried out. In the simulations, the dimensions of the analysis space were 2 m, 6 m, and 2 m in the x, y, and z directions respectively, and the space step was 5 cm. The time step was determined by (14) with $\alpha = 0.001$. All the six boundaries were treated as the 2nd-oreder Liao's absorbing boundary. An earth was placed at the bottom of the analysis space, where its thickness was 10 cm and its resistivity was $\rho_e = 1.69 \times 10^{-8}$ simulating the copper plate. PG was modeled as a z-direction voltage source with its internal resistance 50 Ω in series, of which the waveform was given by a piecewise linear approximation of its open voltage as in Fig. 6 (a). The radius of the horizontal conductor was taken into account by the proposed method in secton II-E [7], although the radius of the vertical lead wire was not considered due to its short length. Figs. 6 (b) and (c) show the measured and calculated waveforms in the case of r = 1.5 cm and h = 50 cm, and the calculated waveforms agree well with measured ones (see Appendix A for more improved result). Fig. 7 is the electric field distribution at t = 20 ns on the conductor $y - z$ plane (a snapshot of its animation

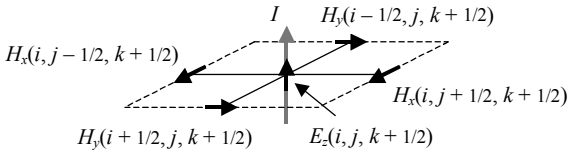

Fig. 3 Calculation of current by Ampere's Law

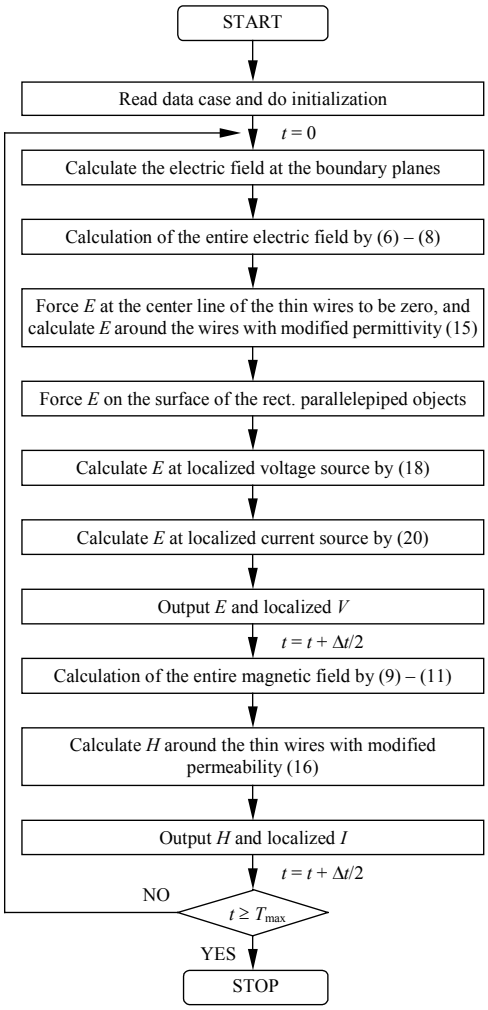

Fig. 4 Calculation process of developed program

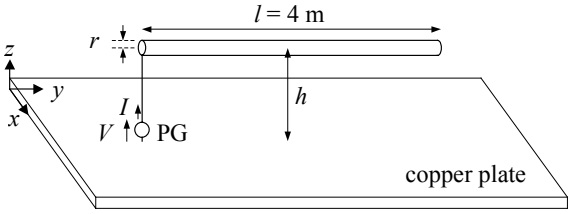

Fig. 5 Conductor arrangement (horizontal conductor system)

visualized by MATLAB). This shows an instance that the reflected wave is about to go back to the sending end.

Fig. 8 shows a comparison of surge impedance between values measured, calculated by the proposed method in sec. II-E, and calculated by Umashankar's method, with varying r and h. The surge impedance was defined as the average value between t = 20 – 25 ns. It is obvious that the proposed method is far more accurate than Umashanlar's method.

B. Vertical Conductor System

The modeling of a vertical conductor is quite important as a basis of transmission tower modeling. Fig. 9 shows a vertical conductor system consisting of four cylindrical pipes each of which the radius is 16.5 mm. This is the same configuration in which a measurement was carried out in [11]. The vertical conductors are excited by a PG via a current leading wire, and the tower-top voltage is defined as the voltage between the tower top and a voltage measuring wire. In the simulation, the dimensions of the analysis space were 9.09 m all in the x, y, and z directions with space step Δs = 10.1 cm. The time step was determined with α = 0.01, and all the six boundaries were treated as the 2nd-order Liao's absorbing boundary. The thickness and the resistivity of the earth were set to 3.03 m and 1.69×10^{-8} Ωm. PG was modeled by a current source with internal resistance 5 kΩ of which the waveform was given in Fig. 10 (a). Figs. 10 (b) and (c) are tower-top voltage and current waveforms, and the calculated results agree well with measured ones. Under a different condition that four 1.01-m vertical grounding electrodes were added to the tower feet in the earth and earth resistivity was set to 100 Ωm, a simulation was carried out. Fig. 11 shows the magnetic field distribution at t = 35.5 ns on the tower $y - z$ plane, when a part of the incoming wave reflects at the earth's surface and the rest penetrates into it.

C. Computation Time

It might be believed that the FDTD method is a time-consuming method. But, the progress of computers in speed and memory is considerable, and a recent personal computer can be used for the FDTD calculations. Actually, the simulations presented in this paper were performed by a personal computer with Pentium III 600 MHz CPU and 256 MB RAM. The computation time of the horizontal conductor case in section II-A was 2 minutes and 53 seconds,

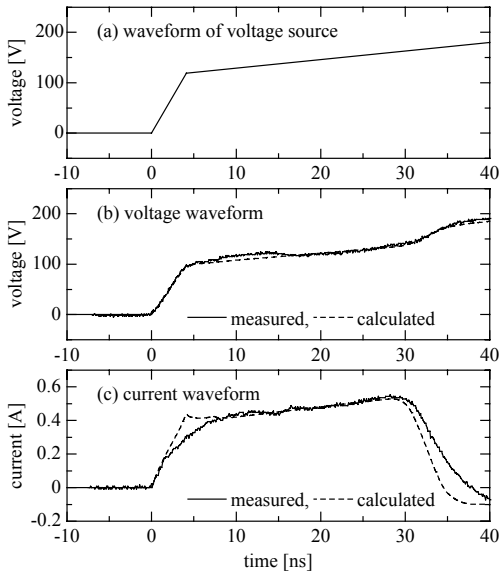

Fig. 6 Calculated and measured waveforms (horizontal conductor system)

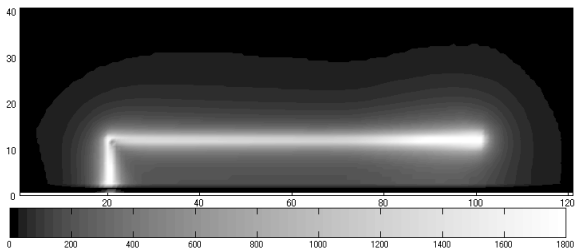

Fig. 7 Electric field strength at t = 20 ns (horizontal conductor system); Electric field strength in [V/m] corresponding to gray scale at the bottom; Unit of vertical and horizontal axes is in cells (Δs = 5 cm)

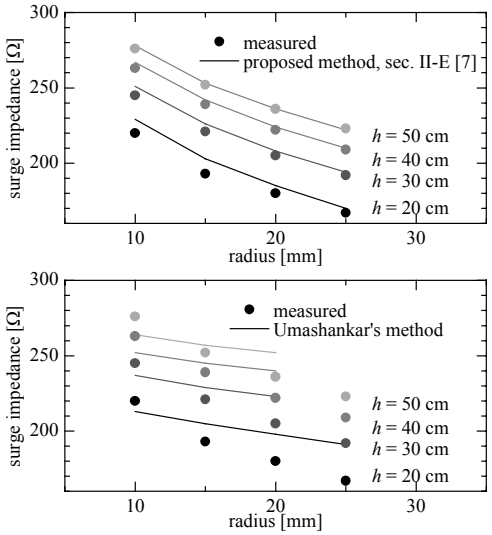

Fig. 8 Comparison between calculated and measured surge impedance, different density (gray scale) indicates different height

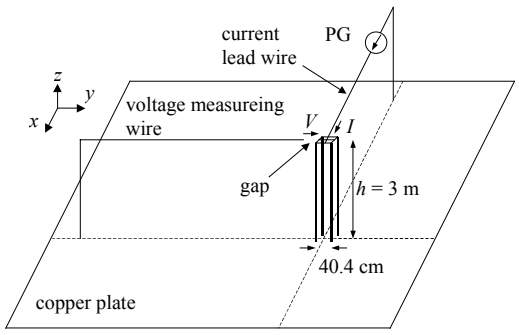

Fig. 9 Conductor arrangement (vertical conductor system)

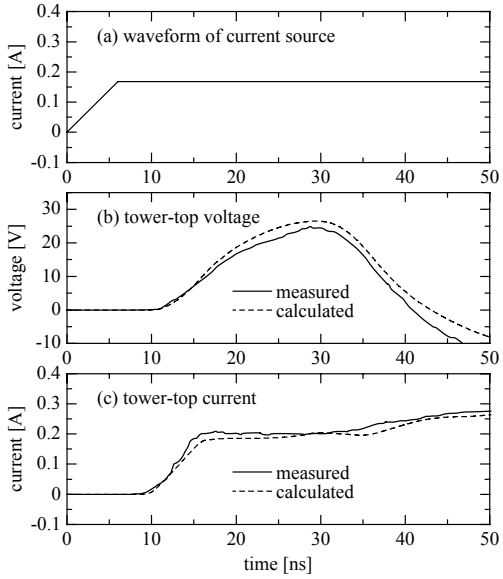

Fig. 10 Calculated and measured waveforms (vertical conductor system)

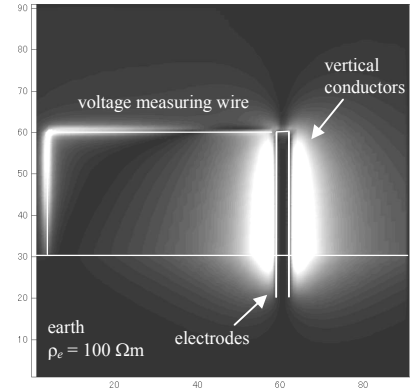

Fig. 11 Magnetic field strength at t = 35.5 ns (vertical conductor system); Expressed by gray-scale gradation from dark black = 0 A/m to clear white = 0.1 A/m; Unit of axes is in cells (Δs = 10.1 cm)

and the vertical conductor case in section II-B 8 minutes and 35 seconds.

V. CONCLUSIONS

In this paper, the development of an FDTD-based surge simulation code VSTL has been described. In the analysis of VSTL, arbitrary number of thin-wire conductors, rectangular-parallelepiped conductors, and localized voltage and current sources are arbitrarily placed in the analysis space, and transient electric and magnetic fields are calculated. Imperfectly-conducting earth and absorbing boundary can also be considered. A method to take into account the radius of a thin wire, which shows more accurate results than a conventional method, has been proposed. The accuracy of VSTL has been validated by comparing with two measured results.

Acknowledgment: The authors are grateful to Mr. Rikido Yonezawa of Tokyo University of Agriculture & Technology and to Mr. Hideki Arai of CRIEPI for their technical assistance. Drs. T. Shindo, Y. Sunaga, and K. Tanabe of CRIEPI are also thanked for their valuable discussions.

REFERENCES

[1] K. S. Yee, "Numerical solution of initial boundary value problems involving Maxwell's equations in isotropic media," *IEEE Trans., Antennas & Propag.*, Vol. AP-14, No. 3, pp. 302 – 307, 1966.

[2] K. S. Kunz, R. J. Luebbers, "The finite difference time domain method for electromagnetics," *CRC Press*, 1993.

[3] K. Tanabe, "A method for computational analysis of transient resistance for grounding systems based on the FD-TD method," *Trans. IEE of Japan*, Vol. 120-B, No. 8/9, pp. 1119 – 1125, 2000.

[4] R. F. Harrington, "Field computation by moment methods," *Macmillan Company*, New York, 1968.

[5] G. J. Burke, A. J. Poggio, "Numerical electromagnetics code (NEC) – method of moments," *Lawrence Livermore Laboratory*, 1981.

[6] G. J. Burke, E. K. Miller, "Modeling antennas near to and penetrating a lossy interface," *IEEE Trans., Antennas & Propag.*, Vol. AP-32, No. 10, pp. 1040 – 1049, 1984.

[7] T. Noda, S. Yokoyama, "Development of a general surge analysis program based on the FDTD method," *Trans. IEE of Japan*, to be published.

[8] Z. P. Liao, H. L. Wong, B.-P. Yang, Y.-F. Yuan, "A transmitting boundary for transient wave analysis," *Science Sinica*, *Series A*, 27, 10, pp. 1063 – 1076, 1984.

[9] K. R. Umashankar, et al., "Calculation and experimental validation of induced currents on coupled wires in an arbitrary shaped cavity," *IEEE Trans., Antennas & Propag.*, AP-35, No. 11, pp. 1248 – 1257, 1987.

[10] T. Kashiwa, S. Tanaka, I. Fukai, "Time domain analysis of Yagi-Uda antennas using the FDTD method," *IEICE Trans.*, B–II, Vol. J76–B–II, No. 11, pp. 872–879, 1993.

[11] T. Hara et al, "Transmission tower model for surge analysis," *Proc. H3 IEE Japan Power & Energy Conf.*, Paper No. II – 270, 1991.

Appendix A

In the horizontal conductor case, the time constant of the CT used in the measurement is 2 ns. Applying the CT response also to the calculated current waveform, Fig. A-1 is obtained, where the CT response is modeled by the 1st-order low-pass filter with τ = 2 ns. With the CT response, the agreement between calculated and measured waveforms is far more improved.

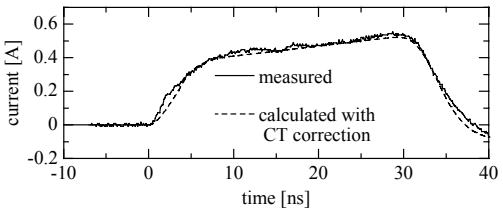

Fig. A-1 Calculated current waveform with CT correction (horizontal conductor system)